

A VINDICATION OF THE RR LYRAE FOURIER LIGHT CURVE DECOMPOSITION FOR THE CALCULATION OF METALLICITY AND DISTANCE IN GLOBULAR CLUSTERS

A. Arellano Ferro

Instituto de Astronomía, Universidad Nacional Autónoma de México, Ciudad Universitaria, México.

Received February 3 2022; accepted April 1 2022

ABSTRACT

We report the mean metallicity and absolute magnitude of RR Lyrae stars in a sample of 37 globular clusters, calculated via the Fourier decomposition of their light curves and *ad hoc* semi-empirical calibrations, in an unprecedented homogeneous approach. This enabled a new discussion of the metallicity dependence of the horizontal branch (HB) luminosity, as a fundamental distance indicator. The calibration for the RRab and RRC stars should be treated separately. For the RRab the dispersion is larger and non-linear. For the RRC stars the correlation is less steep, very tight and linear. The relevance of the HB structural parameter \mathcal{L} , is highlighted and we offer a non-linear calibration of the form $M_V([\text{Fe}/\text{H}], \mathcal{L})$. Excellent agreement is found between values of $[\text{Fe}/\text{H}]$ and M_V from the light curve decomposition with spectroscopic values and distances obtained via Gaia-DR3 and HST. The variables census in 35 clusters includes 326 stars found by our program.

RESUMEN

Reportamos valores medios de la metalicidad y magnitud absoluta de estrellas RR Lyrae en 37 cúmulos globulares (CGs), calculados homogéneamente por medio de la descomposición de Fourier de las curvas de luz y de calibraciones *ad hoc* semi empíricas. Lo anterior permitió un nuevo análisis de la luminosidad de la rama horizontal (RH) y su dependencia de la metalicidad, como indicador fundamental de distancia. La calibración para estrellas RRab y RRC debe tratarse por separado. Para las RRab no es lineal y presenta mayor dispersión. Para las RRC la correlación es lineal y estrecha. La relevancia del parámetro de estructura de la RH, \mathcal{L} para las RRab, es evidente. Ofrecemos una calibración de la forma $M_V([\text{Fe}/\text{H}], \mathcal{L})$. Los valores de $[\text{Fe}/\text{H}]$ y M_V comparan muy bien con valores espectroscópicos y determinaciones de distancia obtenidas con datos de Gaia-DR3 and HST. El censo de variables en 35 cúmulos incluye 326 descubiertas por nuestro programa.

Key Words: globular clusters: general — stars: horizontal branch — stars: distances — stars: fundamental parameters — stars: variables: RR Lyrae

1. A BRIEF PANORAMA OF THE M_V - $[\text{Fe}/\text{H}]$ RELATION

The relevance of RR Lyrae (RRL) stars as distance indicators has been well known since the early 20th century. Shapley (1917) recognized that “the median magnitude of the short-period variables [RR Lyrae stars] apparently has a rigorously constant value in each globular cluster” and “the observed differences in the mean values then become sensitive criteria of distance, and the relative parallaxes of these remote systems can be known with an accu-

racy...”, a fact that was used later by Shapley himself to describe the Galactic distribution of globular clusters (Shapley 1918). This apparently constant value of the mean magnitude of the RRL can now be interpreted as the luminosity level of the horizontal branch (HB) being constant in all globular clusters. The fact that this is not exactly the case, but instead that metallicity plays a role in determining the luminosity level of the HB, has been demonstrated from theoretical and observational grounds. Sandage (1981); Lee et al. (1990); Sandage (1990)

provided a calibration of the M_V -[Fe/H] relation. Lee et al. (1990) discussed its dependence on helium abundance. Other empirical calibrations followed in the works of Walker (1992), Carney et al. (1992), Sandage (1993) and Benedict et al. (2011). Complete summaries on the calibration of the M_V -[Fe/H] relation can be found in the works of Chaboyer (1999), Cacciari & Clementini (2003) and Sandage & Tamman (2006).

While the relation has been considered to be linear in most empirical works, a non-linear nature is advocated by theoretical approaches, e.g. Cassisi et al. (1999) and VandenBerg et al. (2000). A linear relation of the form $M_V = a + b[\text{Fe}/\text{H}]$ has been broadly accepted in the literature and the slope, resulting from a variety of independent calibrations, ranges a wide span (0.13 - 0.30) as different strategies have been adopted, mainly towards the calculation of M_V . The relevance of the slope and zero point of this relation on the relative and absolute ages of the globular clusters has been amply discussed by Chaboyer et al. (1996, 1998) and Demarque et al. (2000). That a linear relation may be an over simplification (Catelan & Smith 2015) becomes very clear from the theoretical analysis of Demarque et al. (2000), that clearly demonstrates the role of the HB structure and that the slope itself is a function of metallicity. The higher complexity of the HB luminosity and metallicity interconnection has however defied clear empirical demonstrations and calibrations, for which, a very extensive and homogeneous endeavor is required.

Our approach to the determination of mean M_V and [Fe/H] of RRL stars has been the Fourier light curve decomposition of both the fundamental mode and first overtone pulsators RRab and RRc respectively. This followed by the employment of solidly established semi-empirical calibrations between the Fourier parameters and the physical quantities. As early as 2002, our group started studying individual clusters in great detail from CCD time-series imaging through the Johnson-Kron-Cousins *VI* bands. Each cluster in the sample has been the subject of a dedicated study, and the discussions include several key aspects of the nature of the globular clusters, such as distinction of likely cluster members from field stars, structure of the colour-magnitude diagram (CMD), pulsating mode distribution on the HB, and theoretical approaches to the mass loss events in the red giant branch and the subsequent mass distribution at the stage of core He-burning (zero age horizontal branch or ZAHB) and post ZAHB evolution.

In 2017, Arellano Ferro et al. (2017) (hereinafter ABG17) summarized the results of a 15-year old program dedicated to study the variable star populations in globular clusters. The program was mainly aimed to the determination of the mean distance and metallicity of the clusters in a homogeneous way, via the Fourier decomposition of the light curves of their RRL stars and the use of well tested semi-empirical calibrations of the Fourier parameters in terms of luminosity and [Fe/H]. The program is based on the Johnson-Kron-Cousins *VI* CCD time-series imaging, and their subsequent scrutiny via the difference images analysis (DIA), that produces accurate photometry even in the crowded central regions of the globular clusters. In the process numerous variables of virtually all types typically present in globular clusters were discovered, of which ABG17 gave a detailed account.

Presently, five years after ABG17 paper, our group has systematically continued enlarging the sample of studied clusters which has increased from 25 to 34. This should enable a better sustained discussion of the M_V -[Fe/H] relation, i.e. the metallicity dependence of the luminosity of the horizontal branch (HB), and the influence of the cluster Oosterhoff type and the HB structure (Demarque et al. 2000). In the present paper we update our discussion of the nature and calibration of the M_V -[Fe/H] relation, and introduce the role of the HB structure parameter \mathcal{L} which is shown to be of obvious relevance. We also perform a census of variable stars per cluster per variable type and reinforce the resulting cluster distance scale from the Fourier approach via the comparison with independent distances recently obtained from *Gaia* and HST accurate data.

We shall mention at this point that the parameters listed in the tables below for specific clusters and number of variables may occasionally differ slightly from the equivalent tables in ABG17, as a result of a critical evaluation of the original samples. The present tables supersede the previous ones.

2. OBSERVATIONS AND IMAGE REDUCTIONS

2.1. Observations

The observations involved in the program have been obtained in several observatories and telescopes in the 0.8-2.15 m range. The majority of the observations have been performed with the 2.0 m Himalayan Chandra Telescope (HCT) of the Indian Astronomical Observatory (IAO), Hanle, India. We have also used the 0.84 m of San Pedro Mártir Observatory (SPM) Mexico, the 2.15 m telescope of the Complejo Astronómico El Leoncito (CASLEO), San Juan, and

the 1.52 m telescope of Bosque Alegre of the Córdoba Observatory, Argentina, the Danish 1.54 m telescope at La Silla, Chile, the SWOPE 1.0 m telescope of Las Campanas Observatory, Chile, the LCOGT 1 m telescope network at the South African Astronomical Observatory (SAAO) in Sutherland, South Africa, at the Side Spring Observatory (SSO) in New South Wales, Australia, and at Cerro Tololo Inter-American Observatory (CTIO), Chile.

2.2. Transformation to the Standard System

All observations have been transformed from the instrumental to the standard Johnson-Kron-Cousins photometric system (Landolt 1992) VI, using local standard stars in the fields of the target clusters. These standard stars have been taken from the extensive collection of Stetson (2000)¹. Typically between 30 and 200 standard stars were available per globular cluster.

2.3. Difference Image Analysis

All the image photometric treatment has been performed using the Difference Image Analysis with the *DanDIA* pipeline (Bramich 2008; Bramich et al. 2013, 2015).

3. CALCULATION OF M_V AND $[Fe/H]$

Our approach to the calculation of mean M_V and $[Fe/H]$ for each GC in the sample has been through the RRL light curve Fourier decomposition, and the application of *ad hoc*, well tested, semi empirical calibrations. The Fourier decomposition of the RRL light curves is performed by fitting the observed light curve in V-band with a Fourier series model of the form:

$$m(t) = A_0 + \sum_{k=1}^N A_k \cos\left(\frac{2\pi}{P} k (t - E) + \phi_k\right), \quad (1)$$

where $m(t)$ is the magnitude at time t , P is the period, and E is the epoch. A linear minimization routine is used to derive the best-fit values of the amplitudes A_k and phases ϕ_k of the sinusoidal components. From the amplitudes and phases of the harmonics in equation 1, the Fourier parameters, defined as $\phi_{ij} = j\phi_i - i\phi_j$, and $R_{ij} = A_i/A_j$, are computed.

Subsequently, the low-order Fourier parameters can be used in combination with semi-empirical calibrations to calculate $[Fe/H]$ and M_V for each RRL,

and hence the mean values of the metallicity and absolute magnitude for the RRL population in the host cluster.

The specific calibrations and zero points used for RRab and RRC stars for this purpose are described in § 3.1. Numerous Fourier decompositions of RRL light curves can be found in the literature. However, over the years, each author has used different calibrations and zero points to estimate M_V and $[Fe/H]$. Our group has also used slightly different equations in the earlier papers but in the work by Arellano Ferro et al. (2010) zero points of the M_V calibrations (see their § 4.2), were discussed and adopted, and we have used them subsequently. In the present paper we have recalculated M_V and $[Fe/H]$ for all clusters in the sample, using the calibrations described in the following section.

The final values found for M_V and $[Fe/H]$, the later expressed in the three different scales defined in § 3.1, are listed in Table 1, which is organized by Oosterhoff types; Oosterhoff (1939, 1944) realized that the periods of fundamental-mode RRL, or RRab stars in a given cluster, group around two values; 0.55 d (Oosterhoff Type I or OoI) and 0.65 d (Oosterhoff Type II or OoII). OoI clusters are systematically more metal-rich than OoII clusters. A third Oosterhoff class (OoIII) (Pritzl et al. 2000), which presently contains only two GCs, NGC 6388 and NGC 6441, is represented by very metal-rich systems, where the periods of their RRab stars average about 0.75 d. A few clusters have been classified as of the intermediate type or OoInt, since the average periods of their RRab stars and their mean $[Fe/H]$ fall between those of Type I and Type II clusters; it has been argued that OoInt clusters may be associated to an extragalactic origin (Catelan 2009) due to their similarity to dSph galaxies, satellites of the Milky Way, and their respective clusters. In Table 1 we include of 16 OoI, 14 OoII, 2 OoIII and 2 OoInt clusters. The calculations have been performed independently for RRab and RRC stars. For clusters with differential reddening, i.e. NGC 1904, NGC 3201, NGC 6333 and NGC 6401, care has been taken in calculating the individual reddening for each RRL. The interested reader is referred to the original papers for a detailed discussion on that subject.

3.1. $[Fe/H]$ and M_V Calibrations

For the calculation of $[Fe/H]$ we adopted the following calibrations:

$$[Fe/H]_j = -5.038 - 5.394P + 1.345\phi_{31}^{(s)}, \quad (2)$$

¹<http://www3.cadc-ccda.hia-ihh.nrc-cnrc.gc.ca/community/STETSON/standards>

TABLE 1
MEAN VALUES OF $[\text{Fe}/\text{H}]$, GIVEN IN THREE DIFFERENT SCALES, AND M_V FROM A
HOMOGENEOUS FOURIER DECOMPOSITION OF THE LIGHT CURVES OF RR LYRAE CLUSTER
MEMBERS¹

GC	Oo	$[\text{Fe}/\text{H}]_{\text{ZW}}$	$[\text{Fe}/\text{H}]_{\text{UV}}$	$[\text{Fe}/\text{H}]_{\text{N}}$	M_V	N	$[\text{Fe}/\text{H}]_{\text{ZW}}$	$[\text{Fe}/\text{H}]_{\text{UV}}$	$[\text{Fe}/\text{H}]_{\text{N}}$	M_V	N	Ref.	$E(B-V)$	\mathcal{L}
NGC (M)		RRab					RRc							
1261	I	-1.48±0.05	-1.38	-1.27	0.59±0.04	6	-1.51±0.13	-1.38	-1.41	0.55±0.02	4	25	0.01	-0.67
1851	I	-1.44±0.10	-1.33	-1.18	0.54±0.03	10	-1.40±0.13	-1.28	-1.28	0.59±0.02	5	23	0.02	-0.20
3201	I	-1.49±0.10	-1.39	-1.29	0.60±0.04	19	-1.47±0.08	-1.37	-1.36	0.58±0.01	2	3	diff.	+0.08
4147	I	-1.56±0.17	-1.47	-1.44	0.57±0.03	5	-1.72±0.26	-1.68	-1.66	0.57±0.05	6	4	0.01	+0.38
5272 (M3)	I	-1.56±0.16	-1.46	-1.46	0.59±0.05	59	-1.65±0.14	-1.57	-1.56	0.56±0.06	23	24	0.01	+0.18
5904 (M5)	I	-1.44±0.09	-1.33	-1.19	0.57±0.08	35	-1.49±0.11	-1.39	-1.38	0.58±0.03	22	19	0.03	+0.31
6171 (M107)	I	-1.33±0.12	-1.22	-0.98	0.62±0.04	6	-1.02±0.18	-0.90	-0.88	0.59±0.03	4	22	0.33	-0.74
6229	I	-1.42±0.07	-1.32	-1.13	0.61±0.06	12	-1.45±0.19	-1.32	-1.58	0.53±0.10	8	20	0.01	+0.14
6362	I	-1.20±0.13	-1.06	-0.73	0.66±0.07	5	-1.21±0.16	-1.09	-1.10	0.59±0.05	6	27	0.06	-0.58
6366	I	-0.84	-0.77	-	0.71	1	-	-	-	-	-	11 ²	0.80	-0.9
6401	I	-1.36±0.09	-1.24	-1.04	0.60±0.07	19	-1.27±0.23	-1.09	-1.16	0.58±0.03	9	21	diff.	+0.13
6712	I	-1.25±0.06	-1.13	-0.82	0.55±0.03	6	-1.10±0.04	-0.95	-0.96	0.57±0.18	3	30	0.35	-0.44
6934	I	-1.56±0.14	-1.46	-1.49	0.58±0.05	15	-1.53±0.12	-1.41	-1.50	0.59±0.03	5	26	0.10	+0.25
6981 (M72)	I	-1.48±0.11	-1.37	-1.28	0.63±0.02	12	-1.66±0.08	-1.60	-1.55	0.57±0.04	4	14	0.06	+0.14
7006	I	-1.51±0.13	-1.40	-1.36	0.61±0.03	31	-1.81±0.27	-1.75	-1.78	0.59±0.04	3	33	0.08	-0.28
Pal13	I	-1.64±0.15	-1.56	-1.67	0.65±0.05	4	-	-	-	-	-	28	0.10	-0.3
288	II	-1.85 ³	-1.87	-1.42	0.38	1	-1.59	-1.52	-1.54	0.58	1	1	0.03	+0.88
1904 (M79)	II	-1.84±0.13 ³	-1.86	-1.46	0.41±0.05	5	-1.71	-1.66	-1.69	0.58	1	2	diff.	+0.74
4590 (M68)	II	-2.07±0.09 ³	-2.21	-2.01	0.49±0.07	5	-2.09±0.03	-2.24	-2.23	0.53±0.01	15	5	0.05	+0.17
5024 (M53)	II	-1.94±0.06 ³	-2.00	-1.68	0.45±0.05	18	-1.84±0.13	-1.85	-1.85	0.52±0.06	3	6	0.02	+0.81
5053	II	-2.05±0.14 ³	-2.18	-2.07	0.46±0.08	3	-2.00±0.18	-2.05	-2.06	0.55±0.05	4	7	0.18	+0.52
5466	II	-2.04±0.14 ³	-2.16	-2.01	0.44±0.09	8	-1.90±0.21	-1.89	-1.96	0.53±0.06	5	8	0.00	+0.58
6205 (M13)	II	-1.60	-1.54	-1.00	0.38	1	-1.70±0.20	-1.63	-1.71	0.59±0.05	3	29	0.02	+0.95
6254 (M10)	II?	-	-	-	-	-	-1.59	-1.52	-1.52	0.52	1	32	0.25	+0.92
6333 (M9)	II	-1.91±0.13 ³	-1.96	-1.72	0.47±0.04	7	-1.71±0.23	-1.66	-1.66	0.55±0.04	6	9	diff.	+0.87
6341 (M92)	II	-2.12±0.18 ³	-2.16 ⁵	-2.26	0.45±0.03	9	-2.01±0.11	-2.11	-2.17	0.53±0.06	3	10	0.02	+0.91
7078 (M15)	II	-2.22±0.19 ³	-2.46	-2.65	0.51±0.04	9	-2.10±0.07	-2.24	-2.27	0.52±0.03	8	15	0.08	+0.67
7089 (M2)	II	-1.60±0.18	-1.51	-1.25	0.53±0.13	10	-1.76±0.16	-1.73	-1.76	0.51±0.08	2	16	0.06	+0.11
7099 (M30)	II	-2.07±0.05 ³	-2.21	-1.88	0.40±0.04	3	-2.03	-2.14	-2.07	0.54	1	17	0.03	+0.77
7492	II	-1.89 ^{3,4}	-1.93	-0.83	0.37	1	-	-	-	-	-	18 ⁵	0.00	+0.76
6402 (M14)	Int	-1.44±0.17	-1.32	-1.17	0.53±0.07	24	-1.23±0.21	-1.12	-1.12	0.58±0.05	36	32	0.57	+0.56
6779 (M56)	Int	-1.76	-1.74	-1.74	0.53	1	-1.96	-2.03	-2.05	0.51	1	34	0.26	+0.82
6388	III	-1.35±0.05	-1.23	-1.00	0.53±0.04	2	-0.67±0.24	-0.64	-0.56	0.61±0.07	6	12	0.40	-0.69
6441	III	-1.35±0.17	-1.23	-0.80	0.43±0.08	7	-1.02±0.34	-0.82	-1.00	0.55±0.08	8	13	0.51	-0.73

Notes: ¹ Quoted uncertainties are 1- σ errors calculated from the scatter in the data for each cluster. The number of stars considered in the calculations is given by N. ² The only RRL V1 is probably not a cluster member. ³ This value has a -0.21 dex added, see § 1 for a discussion. ⁴ Adopted since published Fourier coefficients are insufficient. ⁵ Based on one light curve not fully covered.

References are the source of the Fourier coefficients: 1. Arellano Ferro et al. (2013b); 2. Kains et al. (2012); 3. Arellano Ferro et al. (2014); 4. Arellano Ferro et al. (2018b); 5. Kains et al. (2015); 6. Arellano Ferro et al. (2011); 7. Arellano Ferro et al. (2010); 8. Arellano Ferro et al. (2008b); 9. Arellano Ferro et al. (2013a); 10. Yepez et al. (2020); 11. Arellano Ferro et al. (2008a); 12. Pritzl et al. (2002); 13. Pritzl et al. (2001); 14. Bramich et al. (2011); 15. Arellano Ferro et al. (2006); 16. Lázaro et al. (2006); 17. Kains et al. (2013); 18. Figuera Jaimes et al. (2013); 19. Arellano Ferro et al. (2016); 20. Arellano Ferro et al. (2015b); 21. Tsapras et al. (2017); 22. Deras et al. (2018); 23. Walker (1998); 24. Cacciari et al. (2005); 25. Arellano Ferro et al. (2019); 26. Yepez et al. (2018); 27. Arellano Ferro et al. (2018a); 28. Yepez et al. (2019); 29. Deras et al. (2019); 30. Deras et al. (2020); 31. Arellano Ferro et al. (2020); 32. Yepez et al. (2022); 33. Rojas Galindo et al. (2021); 34. Deras et al. (2022)

$$[\text{Fe}/\text{H}]_{\text{ZW}} = 52.466P^2 - 30.075P + 0.131\phi_{31}^{(c)2} - 0.982\phi_{31}^{(c)} - 4.198\phi_{31}^{(c)}P + 2.424, \quad (3)$$

from Jurcsik & Kovács (1996) and Morgan et al. (2007) for RRab and RRc stars, respectively. In the above equations, $\phi^{(c)}$ and $\phi^{(s)}$ are the phases calculated either on a cosine or a sine series respectively,

and they are correlated as $\phi^{(s)} = \phi^{(c)} - \pi$. The iron abundance on the Jurcsik & Kovács (1996) scale can be converted into the Zinn & West (1984) scale using the equation $[\text{Fe}/\text{H}]_{\text{J}} = 1.431[\text{Fe}/\text{H}]_{\text{ZW}} + 0.88$ (Jurcsik 1995). Then, the $[\text{Fe}/\text{H}]_{\text{ZW}}$ can be transformed into the spectroscopic scale $[\text{Fe}/\text{H}]_{\text{UV}}$ defined by Carretta et al. (2009) from high resolution spec-

troscopic determinations of the iron abundance, via the relation: $[\text{Fe}/\text{H}]_{\text{UV}} = -0.413 + 0.130 [\text{Fe}/\text{H}]_{\text{ZW}} - 0.356 [\text{Fe}/\text{H}]_{\text{ZW}}^2$.

Nemec et al. (2013) calculated non-linear calibrations of $[\text{Fe}/\text{H}]$ in terms of ϕ_{31} and pulsating period, using as calibrators the iron to hydrogen abundances of 26 RRab and 110 RRC stars calculated from high dispersion spectroscopy. For the RRC stars they added four RRC stars to the original 106 used by Morgan et al. (2007) (equation 3), and removed *a posteriori* nine outlier stars. Nemec's calibrations for the RRab and RRC stars are respectively of the form;

$$[\text{Fe}/\text{H}]_{\text{N}} = -8.65 - 40.12P + 5.96\phi_{31}^{(s)}(K) + 6.27\phi_{31}^{(s)}(K)P - 0.72\phi_{31}^{(s)}(K)^2, \quad (4)$$

where $\phi_{31}^{(s)}(K) = \phi_{31}^{(s)} + 0.151$ is given in the *Kepler* scale (Nemec et al. 2013), and

$$[\text{Fe}/\text{H}]_{\text{N}} = 1.70 - 15.67P + 0.20\phi_{31}^{(c)} - 2.41\phi_{31}^{(c)}P + 18.0P^2 + 0.17\phi_{31}^{(c)2}. \quad (5)$$

As pointed out by Nemec et al. (2013), since the above calibrations are based on high resolution spectroscopic determinations of $[\text{Fe}/\text{H}]$, the derived values $[\text{Fe}/\text{H}]_{\text{N}}$ are on the UV scale of Carretta et al. (2009). Thus, they should be comparable to the values $[\text{Fe}/\text{H}]_{\text{UV}}$, a point on which we shall comment below.

For the calculation of M_V we adopted the calibrations:

$$M_V = -1.876 \log P - 1.158A_1 + 0.821A_3 + 0.41, \quad (6)$$

$$M_V = -0.961P - 0.044\phi_{21}^{(s)} - 4.447A_4 + 1.061, \quad (7)$$

from Kovács & Walker (2001) and Kovács & Kanbur (1998) for the RRab and RRC stars, respectively. The zero points of equations 6 and 7 have been calculated to scale the luminosities of RRab and RRC stars to the distance modulus of 18.5 mag for the Large Magellanic Cloud (LMC) (see the discussion in § 4.2 of Arellano Ferro et al. (2010)).

In Table 1 we list the globular clusters studied by our team and the resulting $[\text{Fe}/\text{H}]$ in the scales of Zinn & West (1984), Carretta et al. (2009) and Nemec et al. (2013), i.e. $[\text{Fe}/\text{H}]_{\text{ZW}}$, $[\text{Fe}/\text{H}]_{\text{UV}}$ and $[\text{Fe}/\text{H}]_{\text{N}}$ and M_V , estimated via the Fourier decomposition of the light curves of the RRab and RRC stars. To this end, we have taken the Fourier parameters published in the original papers and applied the above calibrations for the sake of homogeneity. We have also included the two metal-rich

clusters NGC 6388 and NGC 6441 studied by Pritzl et al. (2002, 2001), NGC 1851 (Walker 1998) and NGC 5272 (M3) (Cacciari et al. 2005) since the light curve Fourier decomposition parameters are available in those papers. In order to increase the sample, the clusters NGC 5286, NGC 6266 and NGC 6809, have been added. For these, Fourier-based physical parameters have been reported by Zorotovic et al. (2010), Contreras et al. (2010) and Olech et al. (1999) respectively and the results have been duly transformed to the proper scales by Kains et al. (2012). In all these calculation of the Fourier-based physical parameters, we have systematically avoided clear Blazhko variables or any amplitude modulated stars. All the relevant papers are recorded in the notes to Table 1.

The use of the above equations and their zero points forms the basis of the discussion of the M_V - $[\text{Fe}/\text{H}]$ relation and the cluster distances on a homogeneous scale, which we present in the following sections.

4. VINDICATION OF THE PHOTOMETRIC APPROACH TO THE METALLICITIES

There is absolutely no doubt that the most precise approach to the determination of metallicities of heavenly bodies is via high-resolution spectroscopy. The practical limitations to that technique are several however; to reach deep in magnitude, typical of the HB in most globular clusters, long exposure times with large telescopes are required, making it unaffordable. The spectroscopic values for 19 clusters listed by Carretta et al. (2009) were obtained in numerous previous papers cited by these authors. The analyses were carried on luminous red giants of $V \approx 14 - 16$ mag, i.e. 2-3 magnitudes brighter than RRL stars at the HB, and after an enormous compromise of observational and computational resources. While this situation may change with the advent of in-orbit high resolution spectrographs, the competition for access to the instrumentation will likely remain tough. The photometric approach to the metallicity and luminosity calculation in RRL stars was envisaged in the 1980's (Simon & Teays 1982), and became a popular alternative since it reaches as low as $V \approx 20$ mag with sufficient accuracy with very short exposure times on 1-2 m-class telescopes, enabling the access to larger samples of clusters. The Fourier decomposition approach was further developed to produce the calibrations in § 3 employed in this paper.

Our goal in this section is to compare the photometric values reported in this work with the spectroscopic values of Carretta et al. (2009). Figure 1

shows the photometric based values of $[\text{Fe}/\text{H}]$ in the UV and Nemec scales (Table 1) for the RRab and RRc stars, plotted versus the spectroscopic values given by Carretta et al. (2009). In Panels (a) and (b) it is clear that the comparison is satisfactory for the case of $[\text{Fe}/\text{H}]_{\text{UV}}$. However, for $[\text{Fe}/\text{H}]_{\text{N}}$ the RRab calibration seems to systematically overestimate the metallicity relative to the spectroscopic values. The iron values from Nemec’s calibration for RRc stars also compare well with the spectroscopic values. There is a mild suggestion in both panels (b) and (d) that the calibrations for the RRc stars of equations 3 and 5, which are in fact based on the same set of calibrators, may require a small adjustment of about -0.2 dex for iron values smaller than -2.0 .

5. THE M_V - $[\text{Fe}/\text{H}]$ CORRELATION

It has been argued that equation 2 overestimates $[\text{Fe}/\text{H}]$ for metal-poor clusters. This problem has been addressed by Jurcsik & Kovács (1996), Schwarzenberg-Czerny & Kaluzny (1998), Kovács (2002), Nemec (2004) and Arellano Ferro et al. (2010). It is difficult to quantify a correction to be applied, and it is likely also a function of the metallicity. However, empirical estimations in the above papers point to a value between -0.2 and -0.3 dex on the scale of equation 2. We have adopted -0.3 dex, which on the ZW scale is equivalent to -0.21 dex. Equally difficult is to define a value of $[\text{Fe}/\text{H}]_{\text{ZW}}$ below which the corrections should be applied. Guided by the metallicity values of globular clusters in the spectroscopic scale of Carretta et al. (2009), we estimated that a reasonable limit would be $[\text{Fe}/\text{H}]_{\text{ZW}} < -1.7$. Therefore, the values listed in Table 1 for clusters with $[\text{Fe}/\text{H}]_{\text{ZW}} < -1.7$ dex were obtained by adding -0.21 dex to the value of $[\text{Fe}/\text{H}]_{\text{ZW}}$ found via equation 2. As a consequence the $[\text{Fe}/\text{H}]_{\text{UV}}$ values for these clusters are also affected by this correction. Note that the good comparison between the photometric $[\text{Fe}/\text{H}]_{\text{UV}}$ and the spectroscopic values displayed in Figure 1 (a) was obtained after the application of the correction above.

In Figure 2 we show the distribution of clusters in the M_V - $[\text{Fe}/\text{H}]$ plane obtained from the RRab stars (left panel) and the RRc stars (right panel). In each of these panels we display the resulting distributions for the three involved scales $[\text{Fe}/\text{H}]_{\text{ZW}}$, $[\text{Fe}/\text{H}]_{\text{UV}}$ and $[\text{Fe}/\text{H}]_{\text{N}}$. In the middle and bottom boxes, for the spectroscopic scales $[\text{Fe}/\text{H}]_{\text{UV}}$ and $[\text{Fe}/\text{H}]_{\text{N}}$, we include as reference, in gray colour, two theoretical, non-linear, versions of the M_V - $[\text{Fe}/\text{H}]$ relation of Cassisi et al. (1999) and Vandenberg et al. (2000).

We shall discuss these correlations separately for the RRab and RRc stars.

5.1. From RRab Stars in Globular Clusters

The trend between $[\text{Fe}/\text{H}]$ in all scales and M_V is evident, as much as the large scatter. There are a few outliers, labeled in the figure, that were not considered in the calculations of the fitted regressions (with the exception of M15). However, some evidence of non-linearity is suggested in the central and bottom panels of Figure 2, particularly oriented by the presence of M15 that is the most metal-poor cluster in the sample; hence its relevance. It is also worth noting that Nemec et al. (2013) calibration, equation 4, includes a wider selection of calibrators with metallicities below -2.0 , and as low as $[\text{Fe}/\text{H}] \approx -2.68$ (for star X Ari). Since the number of stars involved in the calculation of the physical parameters varies from cluster to cluster, all the fits below have been weighted by $1/(\sigma_i^2/N_i)$. The quadratic fits for $[\text{Fe}/\text{H}]_{\text{UV}}$ and $[\text{Fe}/\text{H}]_{\text{N}}$ are of the form:

$$M_V = 1.016(\pm 0.170) + 0.428(\pm 0.207)[\text{Fe}/\text{H}]_{\text{UV}} + 0.081(\pm 0.060)[\text{Fe}/\text{H}]_{\text{UV}}^2, \quad (8)$$

with an rms=0.060 mag, and

$$M_V = 0.740(\pm 0.056) + 0.141(\pm 0.077)[\text{Fe}/\text{H}]_{\text{N}} + 0.013(\pm 0.026)[\text{Fe}/\text{H}]_{\text{N}}^2, \quad (9)$$

with an rms=0.060 mag.

The quadratic empirical solutions for $[\text{Fe}/\text{H}]_{\text{UV}}$, shown in Figure 2 (b), is remarkably similar to the theoretical predictions of Vandenberg et al. (2000) and Cassisi et al. (1999), in shape and luminosity level. To our knowledge, this is the first empirical solution that reproduces the theoretical predictions of the non-linear nature of the correlation, which it has likely been enabled by the homogeneous treatment of a large number of clusters, and the distinction of RRab and RRc stars.

We call attention to the inclusion of the metal rich cluster NGC 6366 ($-0.77, 0.71$) in the UV correlation for the RRab, in spite of its metallicity being derived from a single star that might not be a cluster member (Arellano Ferro et al. 2008b). However, excluding it or employing the value $[\text{Fe}/\text{H}]=-0.59$ listed by Harris (1996) makes no significant variation in the correlation.

5.2. From RRc Stars in Globular Clusters

The mean $[\text{Fe}/\text{H}]$ and M_V determined from the RRc stars in the family of studied globular clusters

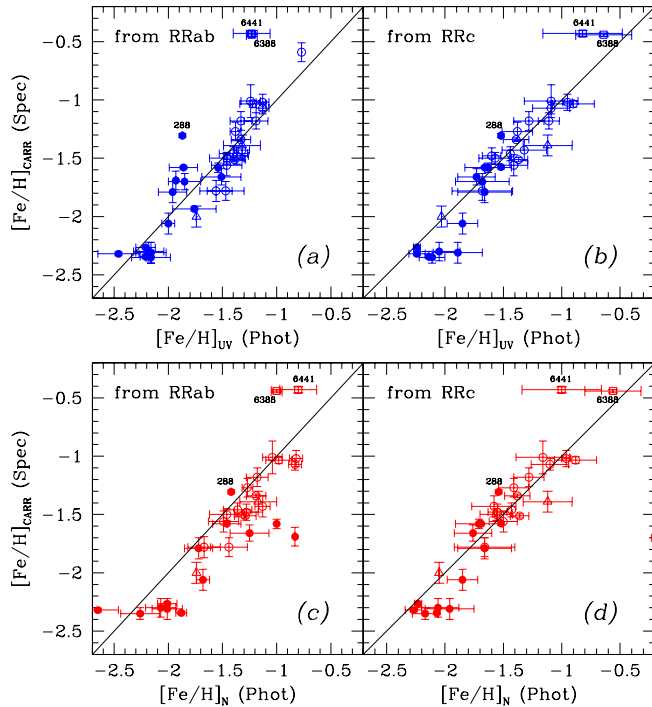


Fig. 1. Comparison of the Fourier based $[\text{Fe}/\text{H}]$ (Table 1), with those from high-resolution spectroscopy based values from Carretta et al. (2009). Filled and empty circles represent OoII and OoI clusters respectively. Open triangles and squares represent OoInt and OoIII clusters. See § 4 for a discussion. The color figure can be viewed online.

are correlated, as shown in the right panel of Figure 2. Immediate differences are seen when compared to the cases from the RRab stars: the slopes are milder, the distributions in the three metallicity scales are all very similar, the correlations are strikingly tight, in spite of which no suggestion of a non-linear correlation is evident. It should also be noted that the Oo-int (triangles) and the OoIII clusters (squares) follow the trends well.

The linear correlations for the $[\text{Fe}/\text{H}]_{\text{UV}}$ and $[\text{Fe}/\text{H}]_{\text{N}}$ can be expressed as:

$$M_V = 0.034(\pm 0.009)[\text{Fe}/\text{H}]_{\text{UV}} + 0.601(\pm 0.015), \quad (10)$$

and

$$M_V = 0.050(\pm 0.004)[\text{Fe}/\text{H}]_{\text{N}} + 0.641(\pm 0.006), \quad (11)$$

with an rms=0.022 mag.

Equations 10 and 11 are basically identical. The reason is that, although the values of $[\text{Fe}/\text{H}]_{\text{UV}}$ and $[\text{Fe}/\text{H}]_{\text{N}}$, come from different formulations (equations 3 and 5), both calibrations come essentially from the same set of calibrator stars, since Nemec et al. (2013) took the calibrators from Morgan et al.

(2007), and added four stars, for a total sample of 101 stars.

The remarkable difference of the cluster distribution on the M_V - $[\text{Fe}/\text{H}]$ plane for the luminosity and metallicity determinations from the Fourier decomposition for RRab and RRc stars, does require some considerations. Naturally one may wonder if this is an artifact of the calibrations employed to transform Fourier parameters into physical parameters. However, the good agreement of the photometric metallicities $[\text{Fe}/\text{H}]_{\text{UV}}$ and the spectroscopic values (Figure 1 (a)), and also the good cluster distance agreement with independent high-quality determinations presented below in § 6, offer support to the photometric calibrations given in § 3 and their results in Table 1. In our opinion, the run of $[\text{Fe}/\text{H}]$ with M_V and the scatter seen in RRab stars are a consequence of the interconnection of the following: RRab stars are larger amplitude variables with a more complex light curve morphology; often the light maximum is very acute, and they are prone to display amplitude and phase modulations. Therefore, their Fourier decomposition is subject to further uncertainties as they require a larger number of harmonics for a proper representation. Their larger periods may also limit a proper coverage of their pul-

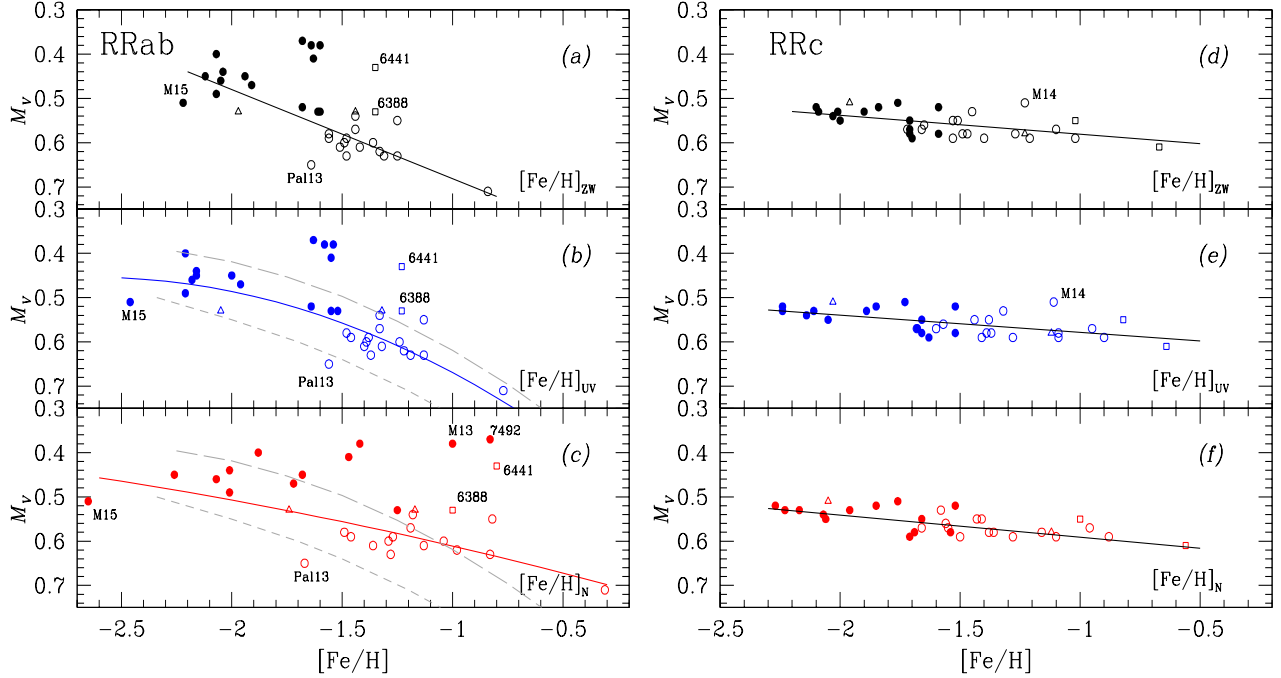


Fig. 2. The $[\text{Fe}/\text{H}]$ versus M_V correlations for RRab and RRC stars. The involved metallicity scale is, from top to bottom panels, $[\text{Fe}/\text{H}]_{\text{ZW}}$, $[\text{Fe}/\text{H}]_{\text{UV}}$ and $[\text{Fe}/\text{H}]_{\text{N}}$. Filled and open circles represent OoII and OoI clusters respectively. Open triangles and squares represent OoInt and OoIII clusters. All fits have been weighted by the number of stars included in each cluster. In the left panel, the gray curves are the theoretical predictions of Cassisi et al. (1999) (long dash) and VandenBerg et al. (2000) (short dash), which are strikingly similar to the photometric solution in panel (b). The color figure can be viewed online.

sating cycle. Also, RRab stars in a given cluster may display small evolutionary stage differences, spreading a luminosity range. These circumstances have their impact on the calibration of the Fourier parameters and on the resultant scatter in the M_V - $[\text{Fe}/\text{H}]$ plane. On the other hand, RRC stars have simpler light curves, mostly sinusoidal, and are more concentrated towards the ZAHB; thus, their Fourier and physical parameters tend to be better correlated.

In summary, the HB luminosity-metallicity correlation seen from the RRab stars is steeper (a fact that had already been reported by ABG17), more scattered and non-linear, whereas from the RRC stars the relation is milder but better defined and linear. RRab and RRC stars should not be mixed for the purpose of studying or applying the correlation as a distance indicator instrument. Therefore, for the sake of estimating a globular cluster distance from its RRL, given its metallicity, one should prefer the RRC stars whenever possible, and either equations 10 or 11.

5.3. The Role of the HB Structure Parameter

Demarque et al. (2000), have argued on theoretical grounds that the overall structure of the HB plays

a relevant role and may be interconnected with the HB luminosity and the metallicity of the parental globular cluster. Here we explore the role of the HB type parameter, or Zinn-Lee parameter, defined as $\mathcal{L} = (B - R)/(B + V + R)$ (Zinn 1986; Lee 1990), from empirical arguments. B , V and R represent the number of stars to the blue of the instability strip (IS), the number of RRL stars, and to the red of the IS respectively. For a better calculation of \mathcal{L} , it is convenient to include, as far as possible, only cluster member stars in the counting. Since the list of \mathcal{L} values for a large number of clusters presented by Torelli et al. (2019) is the result of membership considerations, we have adopted them for the subsequent analysis. When a cluster is not included in the above list we used the value reported by Catelan (2009). The one exception is NGC 7079 (M2). For this cluster, the reported value is $\mathcal{L}=+0.96$. The analysis of the projected positions and proper motions available in the *Gaia*-eDR3 data base, and the application of the method of Bustos Fierro & Calderón (2019), kindly performed by Dr. Bustos Fierro, renders a CMD of very likely cluster member stars, with a substantial population of red HB stars for $\mathcal{L}=+0.34$, which shall

be adopted. For a few other clusters where similar analyses have been carried out, \mathcal{L} values close to those of Torelli et al. (2019) were found.

Figure 3 illustrates the correlation between \mathcal{L} and M_V , the latter as obtained from the Fourier decomposition for RRab stars (top panel) and RRC stars (bottom panel). In the case of the RRab stars the correlation clearly shows a quadratic trend, once the two Oo-Int clusters, NGC 6388 and NGC 6441, were excluded. In the case of the RRC stars the correlation appears linear with a very mild slope. The corresponding fits in Figure 3 are of the form:

$$M_V = 0.620(\pm 0.011) - 0.029(\pm 0.018)\mathcal{L} - 0.135(\pm 0.036)\mathcal{L}^2, \quad (12)$$

with an rms = 0.058, and

$$M_V = 0.558(\pm 0.006) - 0.019(\pm 0.013)\mathcal{L}, \quad (13)$$

with an rms = 0.026.

Considering the trends in Figure 2 for the RRab and RRC, both for the $[\text{Fe}/\text{H}]_{\text{UV}}$ values (middle panels), and in Figure 3, the dependence of M_V on the metallicity $[\text{Fe}/\text{H}]$ and HB structure parameter \mathcal{L} , can be expressed, for the RRab and RRC respectively as:

$$M_V = A + B[\text{Fe}/\text{H}]_{\text{UV}} + C[\text{Fe}/\text{H}]_{\text{UV}}^2 + D\mathcal{L} + E\mathcal{L}^2, \quad (14)$$

with $A=+1.096(\pm 0.141)$, $B=+0.519(\pm 0.172)$, $C=+0.119(\pm 0.050)$, $D=+0.006(\pm 0.014)$, $E=-0.111(\pm 0.029)$, and rms = 0.053 mag.

$$M_V = +0.609(\pm 0.016) + 0.032(\pm 0.009)[\text{Fe}/\text{H}]_{\text{UV}} + 0.015(\pm 0.011)\mathcal{L}, \quad (15)$$

with rms = 0.024 mag.

The equivalent calibrations in terms of the metallicity in the scale of Nemec et al. (2013), $[\text{Fe}/\text{H}]_{\text{N}}$ are:

$$M_V = A + B[\text{Fe}/\text{H}]_{\text{N}} + C[\text{Fe}/\text{H}]_{\text{N}}^2 + D\mathcal{L} + E\mathcal{L}^2, \quad (16)$$

with $A=+0.720(\pm 0.082)$, $B=+0.130(\pm 0.098)$, $C=+0.033(\pm 0.029)$, $D=-0.043(\pm 0.020)$, $E=-0.145(\pm 0.030)$, and rms = 0.055 mag.

$$M_V = +0.655(\pm 0.019) + 0.063(\pm 0.013)[\text{Fe}/\text{H}]_{\text{N}} + 0.012(\pm 0.009)\mathcal{L}, \quad (17)$$

with rms = 0.019 mag.

For the calibration of equations 14 and 16 from the RRab solutions, the terms involving \mathcal{L} are small but significant. On the contrary, equations 15 and

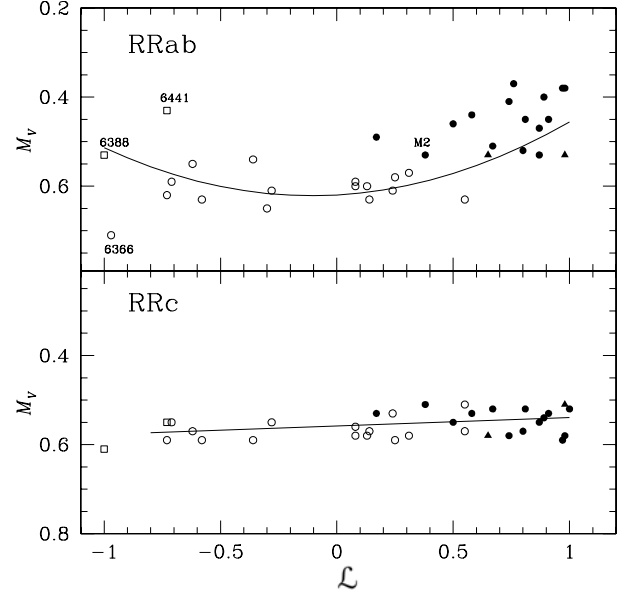


Fig. 3. The HB structure parameter \mathcal{L} vs. mean M_V for a family of clusters coded as in Figure 1. Two open squares for the OoIII clusters were not considered in the weighted fits.

17 from the RRC solutions, the last term is insignificant, and in fact, for instance equations 10 and 15 in the UV scale, or equations 11 and 17 in the Nemec's scale, are, within the uncertainties, indistinguishable, confirming the linearity and sufficiency of an M_V - $[\text{Fe}/\text{H}]$ relation for the RRC stars.

Therefore, the empirical M_V - $[\text{Fe}/\text{H}]$ relation as worked out from the Fourier decomposition of RRab stars light curves, has turned out to be much more complex, with the metallicity and HB structure playing a measurable role, and equations 14 and 16 are a good representation.

For the RRC stars, with simpler light curves and generally being more confined near the ZAHB, the M_V - $[\text{Fe}/\text{H}]$ relation remains linear and simple, and the structure of the HB does not seem to play any pertinent role; equation 10 and 11, or for any purpose equations 15 and 17, are good empirical calibrations, with a well established slope around 0.06.

6. GLOBULAR CLUSTER DISTANCES

Once the mean absolute magnitude M_V for the HB is obtained for a given cluster, its distance can be estimated for an assumed value of $E(B-V)$. Using the values listed in Table 1 the distances were calculated and are listed in Table 2 as they were obtained either for the RRab or RRC stars from equations 6 and 7 respectively. We perform a comparison with accurate mean distances recently estimated

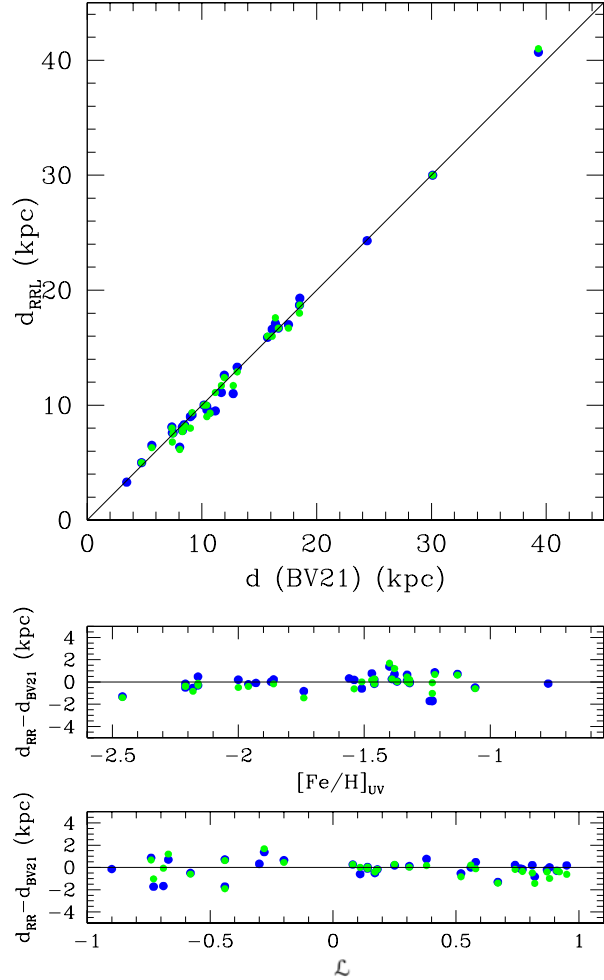


Fig. 4. Comparison of distances obtained from the RRL Fourier decomposition and those of BV21. Blue and green symbols stand for distances derived from RRab and RRc Fourier light curve treatment, respectively. The color figure can be viewed online.

by Baumgardt & Vasiliev (2021) (hereinafter BV21), calculated for a large sample of globular clusters using the data from *Gaia*-eDR3, *HST* and selected literature distances.

It should be obvious from Table 2 that the distances derived from our Fourier approach (Columns 2 and 3) agree with those of BV21. Figure 4 is a graphical comparison and shows how the distance differences do not correlate either with the metallicity or with the HB structure parameter. The Fourier and the BV21 distances differences are all smaller than 1.7 kpc and display a standard deviation of 0.7 kpc.

The agreement is remarkably good considering that the distance determinations come from completely independent approaches. We note that the

distances obtained from the M_V calibrations for RRab and RRc stars, are also independent, as they come from different and independent calibrations. This gives further support to the M_V calibrations of equations 6 and 7 and to their zero points (Arellano Ferro et al. 2010).

The accurate distances of individual globular clusters obtained from the RRL stars listed in Table 4, can serve as a frame of comparison of other independent methods to calculate cluster distances. Given that SX Phe stars are common in globular clusters, they can be used as secondary distance indicators through their well established P-L relation, of which, however, different calibrations are found in the literature. We shall explore the consistency of the results. We considered the calibrations of Arellano Ferro et al. (2011) (AF11), and Cohen & Sarajedini (2012) (CS12). The resulting distances from these two calibrations of 13 clusters with well observed SX Phe stars are listed in Columns 4 and 6 of Table 2, Column 5 indicates the number of member SX Phe stars available in each cluster. We should emphasize that the two calibrations lead to distances agreeing within 1.3 kpc, except for NGC 6934 where the distance differences is ≈ 2.0 kpc for the CS12 calibration. The SX Phe distances agree with the RRL results well within 1 kpc, i.e. the average RRL and SX Phe distance match in average by $\approx 4\%$ of the corresponding distance.

7. VARIABLE STARS IN OUR SAMPLE OF GLOBULAR CLUSTERS

Once a CCD time-series photometry is performed on a given cluster, a by-product of the exercise is the discovery of previously undetected variables. In the work carried by our group, we have systematically searched for variables via a variety of approaches described in the individual papers, e.g. Arellano Ferro et al. (2013b). In Table 3 we summarize the number of variables, and their types, known in the globular clusters of our sample, noting the ones found by our work. We have found 326 new variables in the field of the clusters, 23 of them are either considered field stars or have not been classified. The most numerous families are in order RRab, RRc, SR, SX Phe, eclipsing binaries, CW and double mode RRd stars. The total number of variables detected in these clusters is 2047 but only 1886 are likely to be truly cluster members. Thus, about 16% of the variables in this sample of clusters has been found by our *VI* CCD time-series imaging program.

TABLE 2

DISTANCES FOR A SAMPLE OF GLOBULAR CLUSTERS ESTIMATED HOMOGENEOUSLY FROM THE RRL STARS LIGHT CURVE FOURIER DECOMPOSITIONS

GC NGC(M)	$d(kpc)$ (RRab)	$d(kpc)$ (RRc)	$d(kpc)$ (SX Phe) P-L AF11	No. of SX Phe	$d(kpc)$ (SX Phe) P-L CS12	$E(B - V)$	$d(kpc)$ BV21
288	9.0±0.2	8.0	8.8±0.4	6	9.4±0.6	0.03	8.988
1261	17.1±0.4	17.6±0.7	–	–	–	0.01	16.400
1851	12.6±0.2	12.4±0.2	–	–	–	0.02	11.951
1904 (M79)	13.3±0.4	12.9	–	–	–	0.01	13.078
3201	5.0±0.2	5.0±0.1	4.9±0.3	16	5.2±0.4	dif	4.737
4147	19.3	18.7±0.5	–	–	–	0.02	18.535
4590 (M68)	9.9±0.3	10.0±0.2	9.8±0.5	6	–	0.05	10.404
5024 (M53)	18.7±0.4	18.0±0.5	18.7±0.6	13	20.0±0.8	0.02	18.498
5053	17.0±0.4	16.7±0.4	17.1±1.1	12	17.7±1.2	0.02	17.537
5272	10.0±0.2	10.0±0.4	–	–	–	0.01	10.175
5466	16.6±0.2	16.0±0.6	15.4±1.3	5	16.4±1.3	0.00	16.120
5904 (M5)	7.6±0.2	7.5±0.3	6.7±0.5	3	7.5±0.2	0.03	7.479
6205 (M13)	7.6	6.8±0.3	7.2±0.7	4	–	0.02	7.419
6171	6.5±0.3	6.3±0.2	–	–	–	0.33	5.631
6229	30.0±1.5	30.0±1.1	27.9	1	28.9	0.01	30.106
6254 (M10)	–	4.7	5.2±0.3	15	5.6±0.3	0.25	5.067
6333 (M9)	8.1±0.2	7.9±0.3	–	–	–	dif	8.300
6341 (M92)	8.2±0.2	8.2±0.4	–	–	–	0.02	8.501
6362	7.8±0.1	7.7±0.2	7.1±0.2	6	7.6±0.2	0.09	8.300
6366	3.3	–	–	–	–	0.80	3.444
6388	9.5±1.2	11.1±1.1	–	–	–	0.40	11.171
6401	6.35±0.7	6.15±1.4	–	–	–	dif	8.064
6402 (M14)	9.1±0.9	9.3±0.5	–	–	–	0.57	9.144
6441	11.0±1.8	11.7±1.0	–	–	–	0.51	12.728
6712	8.1±0.2	8.0±0.3	–	–	–	0.35	7.382
6779 (M56)	9.6	9.0	–	–	–	0.26	10.430
6934	15.9±0.4	16.0±0.6	15.8	1	18.0	0.10	15.716
6981 (M72)	16.7±0.4	16.7±0.4	16.8±1.6	3	18.0±1.0	0.06	16.661
7006	40.7±1.6	41.0±1.6	–	–	–	0.08	39.318
7078 (M15)	9.4±0.4	9.3±0.6	–	–	–	0.08	10.709
7089 (M2)	11.1±0.6	11.7±0.02	–	–	–	0.06	11.693
7099 (M30)	8.32±0.3	8.1	8.0	1	8.3	0.03	8.458
7492	24.3	–	22.1±3.2	2	24.1±3.7	0.00	24.390
Pal 13	23.8±0.6	–	–	–	–	0.10	23.475

8. CONCLUSIONS

A homogeneous approach towards the determination of mean M_V and $[Fe/H]$ from the Fourier decomposition of the cluster member RRL light curves, enables a new empirical exploration of the nature of the M_V - $[Fe/H]$ relation, which describes the dependence of the luminosity of the HB on the metallicity. Although numerous efforts, from assorted strategies, have been performed to establish the zero point and slope of the relation, universal values have been elusive. We found that, if the RRL stars are to be used as indicators of the form of the relation, or if this is to be employed as a distance indicator instrument, it should be treated independently for RRab and RRc stars. The reason is that the relation displays a different nature; for the RRab stars it is non linear with considerable scatter, while for the RRc it is tight, linear and the slope is mild.

Following the suggestion of theoretical works (Demarque et al. 2000), the inclusion of the HB structural parameter \mathcal{L} demonstrates that M_V is also correlated with \mathcal{L} , in a nonlinear fashion for the RRab analysis. For the RRc the role of \mathcal{L} is negligible. We offer a calibration M_V - $[Fe/H]$ - \mathcal{L} , with $[Fe/H]$ in the spectroscopic scale of Carretta et al. (2009) (equation 14) or in the Nemeč et al. (2013) scale (equation 16) valid for RRab stars, and linear calibrations M_V - $[Fe/H]$ in the above two scales (equation 10 or equation 11) valid for RRc stars.

We find pertinent at this point to recall a well established result: that globular clusters harbour more than one generation of stars (e.g. Bedin et al. 2004; Piotto et al. 2005, 2007), and that each generation has a measurable different chemical abundance; particularly, the He content increases in later generations (Milone et al. 2018). As a result of different evolutionary sequences, the objects on the HB

TABLE 3
 NUMBER OF PRESENTLY KNOWN VARIABLES PER CLUSTER FOR THE MOST COMMON
 VARIABLE TYPES, IN A SAMPLE OF GLOBULAR CLUSTERS STUDIED BY OUR GROUP[†]

GC NGC (M)	RRab	RRc	RRd	SX Phe	Binaries	CW-(AC)-RV	SR, L,M	Spotted	Unclass others *	Total per cluster	Ref.
288	0/1	0/1	0/0	0/6	0/1	0/0	0/1			0/10	1
1261	0/16	0/6	0/0	0/3	0/1	0/0	0/3			0/29	22
1904 (M79)	0/6	1/5	0/0	0/5	0/1	0/1	0/14		0/1	1/32	
3201	0/72	0/7	0/0	3/24	0/11	0/0	0/8	0/2	0/7	3/124	3
4147	0/5	0/19	0/1	0/0	0/14	0/0	2/2		0/3	2/41	4,23,35
4590 (M68)	0/14	0/16	0/12	4/6	0/0	0/0	0/0		1/2	4/48	5
5024 (M53)	0/29	2/35	0/0	13/28	0/0	0/0	1/12			16/104	6,7
5053	0/6	0/4	0/0	0/5	0/0	0/0	0/0			0/15	8
5466	0/13	0/8	0/0	0/9	0/3	0/1	0/0		2/2	0/34	9
5904 (M5)	2/89	1/40	0/0	1/6	1/3	0/2	11/12		0/1	16/152	17,18
6171 (M107)	0/15	0/6	0/0	0/1	0/0	0/0	2/3		0/3	2/25	24
6205 (M13)	0/1	1/7	2/2	2/6	1/3	0/3	3/22		0/4	9/44	25
6229	10/42	5/15	0/0	1/1	0/0	2/5	6/6		0/1	24/69	19
6254 (M10)	0/0	0/1	0/0	1/15	2/10	0/3	0/5		0/2	3/34	26
6333 (M9)	0/8	2/10	1/1	0/0	3/4	1/1	5/6		3/4	12/30	10
6341 (M92)	0/9	0/5	1/1	1/6	0/0	0/1	1/1		0/6	3/23	27
6362	0/16	0/15	1/3	0/6	0/12	0/0	0/0	0/3	0/22	1/55	28
6366	0/1	0/0	0/0	1/1	1/1	1/1	3/4			6/8	11
6388	1/14	2/23	0/0	0/1	0/10	1/11	42/58			46/117	21
6397	0/0	0/0	0/0	0/5	0/15	0/0	0/1		0/13	0/21	29
6401	6/23	6/11	0/0	0/0	0/14	0/1	3/3		14/14	15/52	20
6402 (M14)	0/55	3/56	1/1	1/1	0/3	0/6	18/32			23/154	30
6441	2/50	0/28	0/1	0/0	0/17	2/9	43/82		0/10	47/187	21
6528	1/1	1/1	0/0	0/0	1/1	0/0	4/4			7/7	21
6638	3/10	2/18	0/0	0/0	0/0	0/0	3/9		0/25	8/37	21
6652	0/3	0/1	0/0	0/0	1/2	0/1	0/2		1/5	1/9	21
6712	0/10	0/4	0/0	0/0	2/2	0/0	5/11		0/8	7/27	31
6779 (M56)	0/1	0/2	0/0	1/1	3/3	0/2	0/3		1/6	4/12	32
6934	3/68	0/12	0/0	3/4	0/0	2/3	3/5		1/6	11/92	33
6981 (M72)	8/37	3/7	0/0	3/3	0/0	0/0	0/1			14/48	12
7078 (M15)	0/65	0/67	0/32	0/4	0/3	0/2	0/3		0/11	0/176	13
7089 (M2)	5/23	3/15	0/0	0/2	0/0	0/4	0/0		0/12	8/44	14
7099 (M30)	1/4	2/2	0/0	2/2	1/6	0/0	0/0		0/3	6/14	17
7492	0/1	0/2	0/0	2/2	0/0	0/0	1/2			3/7	16
Pal 13	0/4	0/0	0/0	0/0	0/0	0/0	1/1			1/5	34
Total per type	41/713	35/448	6/54	39/153	16/140	9/57	157/316	0/5	23/161	303/1886	

[†]The variable star types are adopted from the General Catalog of Variable Stars (Kazarovets et al. 2009; Samus et al. 2009). Entries expressed as M/N indicate the M variables found or reclassified by our program and the total number N of presently known variables. Column 11 indicates the relevant papers on a given clusters.

*Numbers from this column are not considered in the totals. Here we include unclassified variables or likely field variables in the FoV of the cluster.

References: 1. Arellano Ferro et al. (2013a); 2. Kains et al. (2012); 3. Arellano Ferro et al. (2014a); 4. Arellano Ferro et al. (2004); 5. Kains et al. (2015); 6. Arellano Ferro et al. (2011); 7. Bramich & Freudling (2012); 8. Arellano Ferro et al. (2010); 9. Arellano Ferro et al. (2008a), 10. Arellano Ferro et al. (2013a), 11. Arellano Ferro et al. (2008b), 12. Bramich et al. (2011); 13. Arellano Ferro et al. (2006); 14. Lázaro et al. (2006); 15. Kains et al. (2013); 16. Figuera Jaimes et al. (2013); 17. Arellano Ferro et al. (2015a), 18. Arellano Ferro et al. (2016); 19. Arellano Ferro et al. (2015b); 20. Tsapras et al. (2017); 21. Skottfelt et al. (2015); 22. Arellano Ferro et al. (2019); 23. Arellano Ferro et al. (2018b); 24. Deras et al. (2018); 25. Deras et al. (2019); 26. Arellano Ferro et al. (2020); 27. Yepez et al. (2020); 28. Arellano Ferro et al. (2018a); 29. Ahumada et al. (2021); 30. Yepez et al. (2022); 31. Deras et al. (2020); 32. Deras et al. (2022); 33. Yepez et al. (2018); 34. Yepez et al. (2019); 35. Lata et al. (2019).

have a large range of He abundance causing the observed HB structure, particularly the color range, and the breadth; the higher the value of Y, the more luminous the corresponding ZAHB would be. Recently it has been shown that small variations in the He-burning core mass would also contribute to

the observed breadth of the HB (Yepez et al. 2022). Hence, the values of the \mathcal{L} parameter employed in the present investigation may be responding to these effects, which in turn may be responsible, at least partially, of the scatter observed in the correlations. Therefore, while it is helpful to identify the cluster

star members, as we have done, the identification of stars belonging to the different generations in each cluster might offer an important improvement on the calibration of the M_V -[Fe/H]- \mathcal{L} correlation.

To give support to our results, we compared the Fourier determinations of [Fe/H] with the spectroscopic values in the scale of Carretta et al. (2009) and found them to be in excellent agreement. The distances obtained from the mean Fourier M_V calibrations, and their zero points, have proven to match within 1.7 kpc and to display a difference dispersion with an rms of 0.7 kpc, with the independent and also homogeneous distances determined by Baumgardt & Vasiliev (2021) from *Gaia*-eDR3 and HST data.

The CCD time-series photometric study of globular clusters, in combination with difference image analysis, has been very fruitful in the discovery of new variables. Following the latest version of the Catalogue of Variable Stars in Globular Clusters (Clement et al. 2001), we updated in Table 3 the number of known variables per type and per cluster and indicated the numbers of variables found and classified by our program over the years, for a total of 303 out of the 1886 variables, likely to be cluster members, presently known in the family of the 35 clusters considered.

I am indebted to all my colleagues that have coauthored the numerous papers cited here, for their sincere dedication and implementation of their expertise to the several astrophysical fronts involved in the project. My special thanks to Prof. Sunetra Giridhar and Dr. Dan Bramich for extended discussions and very useful suggestions. A warm acknowledgement to Dr. Ivan Bustos Fierro for his willingness to decipher the stellar membership status in several clusters. I recognize with gratitude the many corrections and comments made by a very attentive anonymous referee, which triggered relevant modifications in the manuscripts. I am grateful to the institutions operating the employed telescopes for the time granted to our project, and to the many support staff members in all these observatories for making possible and efficient all our data gathering. The facilities at IAO and CREST are operated by the Indian Institute of Astrophysics, Bangalore. The project has been generously supported through the years by the program PAPIIT of the DGAPA-UNAM, México via several grants, the most recent being IG100620.

DATA AVAILABILITY

The data underlying this article shall be made available on request to the author (armando@astro.unam.mx).

REFERENCES

- Ahumada, J. A., Arellano Ferro, A., Bustos Fierro, I. H., et al. 2021, *New A*, 88, 101607, <https://doi.org/10.1016/j.newast.2021.101607>
- Arellano Ferro, A., Ahumada, J. A., Bustos Fierro, I. H., Calderón, J. H., & Morrell, N. I. 2018a, *AN*, 339, 183, <https://doi.org/10.1002/asna.201813465>
- Arellano Ferro, A., Ahumada, J. A., Calderón, J. H., & Kains, N. 2014, *RMxAA*, 50, 307
- Arellano Ferro, A., Bramich, D. M., Figuera Jaimes, R., et al. 2013a, *MNRAS*, 434, 1220, <https://doi.org/10.1093/mnras/stt1080>
- Arellano Ferro, A., Bramich, D. M., Giridhar, S., et al. 2013b, *AcA*, 63, 429
- Arellano Ferro, A., Bramich, D. M., & Giridhar, S. 2017, *RMxAA*, 53, 121
- Arellano Ferro, A., Bramich, D. M., Giridhar, S., Luna, A., & Muneer, S. 2015a, *IBVS*, 6137, 1
- Arellano Ferro, A., Bustos Fierro, I. H., Calderón, J. H., & Ahumada, J. A. 2019, *RMxAA*, 55, 337, <https://doi.org/10.22201/ia.01851101p.2019.55.02.18>
- Arellano Ferro, A., Figuera Jaimes, R., Giridhar, S., et al. 2011, *MNRAS*, 416, 2265, <https://doi.org/10.1111/j.1365-2966.2011.19201.x>
- Arellano Ferro, A., García Lugo, G., & Rosenzweig, P. 2006, *RMxAA*, 42, 75
- Arellano Ferro, A., Giridhar, S., & Bramich, D. M. 2010, *MNRAS*, 402, 226, <https://doi.org/10.1111/j.1365-2966.2009.15931.x>
- Arellano Ferro, A., Giridhar, S., Rojas López, V., et al. 2008a, *RMxAA*, 44, 365
- Arellano Ferro, A., Luna, A., Bramich, D. M., et al. 2016, *Ap&SS*, 361, 175, <https://doi.org/10.1007/s10509-016-2757-5>
- Arellano Ferro, A., Mancera Piña, P. E., Bramich, D. M., et al. 2015b, *MNRAS*, 452, 727, <https://doi.org/10.1093/mnras/stv1299>
- Arellano Ferro, A., Rojas Galindo, F. C., Muneer, S., & Giridhar, S. 2018b, *RMxAA*, 54, 325
- Arellano Ferro, A., Rojas López, V., Giridhar, S., & Bramich, D. M. 2008b, *MNRAS*, 384, 1444, <https://doi.org/10.1111/j.1365-2966.2007.12760.x>
- Arellano Ferro, A., Yepez, M. A., Muneer, S., et al. 2020, *MNRAS*, 499, 4026, <https://doi.org/10.1093/mnras/staa2977>
- Baumgardt, H. & Vasiliev, E. 2021, *MNRAS*, 505, 5957, <https://doi.org/10.1093/mnras/stab1474>
- Bedin, L. R., Piotto, G., Anderson, J., et al. 2004, *ApJ*, 605, 125, <https://doi.org/10.1086/420847>

- Benedict, G. F., McArthur, B. E., Feast, M. W., et al. 2011, *AJ*, 142, 187, <https://doi.org/10.1088/0004-6256/142/6/187>
- Bramich, D. M. 2008, *MNRAS*, 386, 77, <https://doi.org/10.1111/j.1745-3933.2008.00464.x>
- Bramich, D. M., Bachelet, E., Alsubai, K. A., Mislis, D., & Parley, N. 2015, *A&A*, 577, 108, <https://doi.org/10.1051/0004-6361/201526025>
- Bramich, D. M., Figuera Jaimes, R., Giridhar, S., & Arellano Ferro, A. 2011, *MNRAS*, 413, 1275, <https://doi.org/10.1111/j.1365-2966.2011.18213.x>
- Bramich, D. M. & Freudling, W. 2012, *MNRAS*, 424, 1584, <https://doi.org/10.1111/j.1365-2966.2012.21385.x>
- Bramich, D. M., Horne, K., Albrow, M. D., et al. 2013, *MNRAS*, 428, 2275, <https://doi.org/10.1093/mnras/sts184>
- Bustos Fierro, I. H. & Calderón, J. H. 2019, *MNRAS*, 488, 3024, <https://doi.org/10.1093/mnras/stz1879>
- Cacciari, C. & Clementini, G. 2003, *Stellar Candles for the Extragalactic Distance Scale*, ed. D. Alloin and W. Gieren, *LNP*, 635, 105
- Cacciari, C., Corwin, T. M., & Carney, B. W. 2005, *AJ*, 129, 267, <https://doi.org/10.1086/426325>
- Carretta, E., Bragaglia, A., Gratton, R., D’Orazi, V., & Lucatello, S. 2009, *A&A*, 508, 695, <https://doi.org/10.1051/0004-6361/200913003>
- Cassisi, S., Castellani, V., degl’Innocenti, S., Salaris, M., & Weiss, A. 1999, *A&AS*, 134, 103, <https://doi.org/10.1051/aas:1999126>
- Catelan, M. 2009, *Ap&SS*, 320, 261, <https://doi.org/10.1007/s1059-009-9987-8>
- Catelan, M. & Smith, H. A. 2015, *Pulsating Stars* (Weinheim, Germany: Wiley-VCH Verlag GmbH & Co)
- Chaboyer, B. 1999, *Globular Cluster Distance Determinations in Post-Hipparcos Cosmic Candles*, ed. A. Heck & F. Caputo (Boston, MA: Kluwer Academic Publishers), 111, https://doi.org/10.1007/978-94-011-4734-7_7
- Chaboyer, B., Demarque, P., Kernan, P. J., & Krauss, L. M. 1998, *ApJ*, 494, 96, <https://doi.org/10.1086/305201>
- Chaboyer, B., Demarque, P., & Sarajedini, A. 1996, *ApJ*, 459, 558, <https://doi.org/10.1086/176921>
- Clement, C. M., Muzzin, A., Dufton, Q., et al. 2001, *AJ*, 122, 2587, <https://doi.org/10.1086/323719>
- Cohen, R. E. & Sarajedini, A. 2012, *MNRAS*, 419, 342, <https://doi.org/10.1111/j.1365-2966.2011.19697.x>
- Contreras, R., Catelan, M., Smith, H. A., et al. 2010, *AJ*, 140, 1766, <https://doi.org/10.1088/0004-6256/140/6/1766>
- Demarque, P., Zinn, R., Lee, Y.-W., & Yi, S. 2000, *AJ*, 119, 1398, <https://doi.org/10.1086/301261>
- Deras, D., Arellano Ferro, A., Bustos Fierro, I. H., & Yezpez, M. A. 2022, *RMxAA*, 58, 121, <https://doi.org/10.22201/ia.01851101p.2022.58.01.10>
- Deras, D., Arellano Ferro, A., Lázaro, C., et al. 2019, *MNRAS*, 486, 2791, <https://doi.org/10.1093/mnras/stz642>
- _____. 2020, *MNRAS*, 493, 1996, <https://doi.org/10.1093/mnras/staa196>
- Deras, D., Arellano Ferro, A., Muneer, S., Giridhar, S., & Michel, R. 2018, *AN*, 339, 603, <https://doi.org/10.1002/asna.201813489>
- Figuera Jaimes, R., Arellano Ferro, A., Bramich, D. M., Giridhar, S., & Kuppuswamy, K. 2013, *A&A*, 556, 20, <https://doi.org/10.1051/0004-6361/201220824>
- Harris, W. E. 1996, *AJ*, 112, 1487, <https://doi.org/10.1086/118116>
- Jurcsik, J. & Kovács, G. 1996, *A&A*, 312, 111
- Kains, N., Arellano Ferro, A., Figuera Jaimes, R., et al. 2015, *A&A*, 578, 128, <https://doi.org/10.1051/0004-6361/201424600>
- Kains, N., Bramich, D. M., Arellano Ferro, A., et al. 2013, *A&A*, 555, 36, <https://doi.org/10.1051/0004-6361/201321819>
- Kains, N., Bramich, D. M., Figuera Jaimes, R., et al. 2012, *A&A*, 548, 92, <https://doi.org/10.1051/0004-6361/201220217>
- Kovács, G. 2002, *ASPC 265, Omega Centauri, A Unique Window into Astrophysics*, ed. F. van Leeuwen, J. D. Hughes, & G. Piotto (San Francisco, CA: ASPC), 163
- Kovács, G. & Kanbur, S. M. 1998, *MNRAS*, 295, 834, <https://doi.org/10.1046/j.1365-8711.1998.01271.x>
- Kovács, G. & Walker, A. R. 2001, *A&A*, 374, 264, <https://doi.org/10.1051/0004-6361:20010844>
- Landolt, A. U. 1992, *AJ*, 104, 340, <https://doi.org/10.1086/116242>
- Lata, S., Pandey, A. K., Pandey, J. C., et al. 2019, *AJ*, 158, 51, <https://doi.org/10.3847/1538-3881/ab22a6>
- Lázaro, C., Arellano Ferro, A., Arévalo, M. J., et al. 2006, *MNRAS*, 372, 69, <https://doi.org/10.1111/j.1365-2966.2006.10742.x>
- Lee, Y.-W. 1990, *ApJ*, 363, 159, <https://doi.org/10.1086/169326>
- Lee, Y.-W., Demarque, P., & Zinn, R. 1990, *ApJ*, 350, 155, <https://doi.org/10.1086/168370>
- Milone, A. P., Marino, A. F., Renzini, A., et al. 2018, *MNRAS*, 481, 5098, <https://doi.org/10.1093/mnras/sty2573>
- Morgan, S. M., Wahl, J. N., & Wieckhorst, R. M. 2007, *MNRAS*, 374, 1421, <https://doi.org/10.1111/j.1365-2966.2006.11247.x>
- Nemec, J. M. 2004, *AJ*, 127, 2185, <https://doi.org/10.1086/382903>
- Nemec, J. M., Cohen, J. G., Ripepi, V., et al. 2013, *ApJ*, 773, 181, <https://doi.org/10.1088/0004-637x/773/2/181>
- Olech, A., Kaluzny, J., Thompson, I. B., et al. 1999, *AJ*, 118, 442, <https://doi.org/10.1086/300917>
- Piotto, G., Bedin, L. R., Anderson, J., et al. 2007, *ApJ*, 661, 53, <https://doi.org/10.1086/518503>

- Piotto, G., Villanova, S., Bedin, L. R., et al. 2005, *ApJ*, 621, 777, <https://doi.org/10.1086/427796>
- Pritzl, B. J., Smith, H. A., Catelan, M., & Sweigart, A. V. 2001, *AJ*, 122, 2600, <https://doi.org/10.1086/323447>
- _____. 2002, *AJ*, 124, 949, <https://doi.org/10.1086/341381>
- Rojas Galindo, F., Arellano Ferro, A., Bustos Fierro, I. H., & Yepez, M. A. 2021, in prep
- Sandage, A. 1981, *ApJ*, 248, 161, <https://doi.org/10.1086/159140>
- _____. 1990, *ApJ*, 350, 631, <https://doi.org/10.1086/168416>
- Sandage, A. & Tammann, G. A. 2006, *ARA&A*, 44, 93, <https://doi.org/10.1146/annurev.astro.43.072103.150612>
- Schwarzenberg-Czerny, A. & Kaluzny, J. 1998, *MNRAS*, 300, 251, <https://doi.org/10.1046/j.1365-8711.1998.01895.x>
- Shapley, H. 1917, *PNAS*, 3, 479, <https://doi.org/10.1073/pnas.3.7.479>
- _____. 1918, *ApJ*, 48, 154, <https://doi.org/10.1086/142423>
- Simon, N. R. & Teays, T. J. 1982, *ApJ*, 261, 586, <https://doi.org/10.1086/160369>
- Skottfelt, J., Bramich, D. M., Figuera Jaimes, J. R., et al. 2015, *A&A*, 573, 103, <https://doi.org/10.1051/0004-6361/201424967>
- Stetson, P. B. 2000, *PASP*, 112, 925, <https://doi.org/10.1086/316595>
- Torelli, M., Iannicola, G., Stetson, P. B., et al. 2019, *A&A*, 629, 53, <https://doi.org/10.1051/0004-6361/201935995>
- Tsapras, Y., Arellano Ferro, A., Bramich, D. M., et al. 2017, *MNRAS*, 465, 2489, <https://doi.org/10.1093/mnras/stw2773>
- VandenBerg, D. A., Swenson, F. J., Rogers, F. J., Iglesias, C. A., & Alexander, D. R. 2000, *ApJ*, 532, 430, <https://doi.org/10.1086/308544>
- Walker, A. R. 1992, *ApJ*, 390, 81, <https://doi.org/10.1086/186377>
- _____. 1998, *AJ*, 116, 220, <https://doi.org/10.1086/300432>
- Yepez, M. A., Arellano Ferro, A., & Deras, D. 2020, *MNRAS*, 494, 3212, <https://doi.org/10.1093/mnras/staa637>
- Yepez, M. A., Arellano Ferro, A., Deras, D., et al. 2022, arXiv e-prints, arXiv:2201.02160, <https://doi.org/10.48550/arXiv.2201.02160>
- Yepez, M. A., Arellano Ferro, A., Muneer, S., & Giridhar, S. 2018, *RMxAA*, 54, 15
- Yepez, M. A., Arellano Ferro, A., Schröder, K.-P., et al. 2019, *NewA*, 71, 1, <https://doi.org/10.1016/j.newast.2019.02.006>
- Zinn, R. 1987, *Stellar Populations*, ed. C. A. Norman, A. Renzini, & M. Tosi (New York, NY: CUP), 73
- Zinn, R. & West, M. J. 1984, *ApJS*, 55, 45, <https://doi.org/10.1086/190947>
- Zorotovic, M., Catelan, M., Smith, H. A., et al. 2010, *AJ*, 139, 357, <https://doi.org/10.1088/0004-6256/139/2/357>